

Synthesis, Molecular Structure, and Catalytic Potential of the Tetrairon Complex $[\text{Fe}_4(\text{N}_3\text{O}_2\text{-L})_4(\mu\text{-O})_2]^{4+}$ (L = 1-Carboxymethyl-4,7-dimethyl-1,4,7-triazacyclononane)

Vladimir B. Romakh,[†] Bruno Therrien,[†] Georg Süss-Fink,^{*,†} and Georgiy B. Shul'pin[‡]

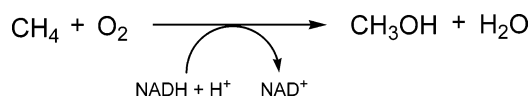
Institut de Chimie, Université de Neuchâtel, CH-2009 Neuchâtel, Switzerland, and Semenov Institute of Chemical Physics, Russian Academy of Sciences, Moscow 119991, Russia

Received November 20, 2006

The reaction of iron sulfate with 1-carboxymethyl-4,7-dimethyl-1,4,7-triazacyclononane (L) and hydrogen peroxide in aqueous ethanol gives a brown dinuclear complex considered to be $[\text{Fe}_2(\text{N}_3\text{O-L})_2(\mu\text{-O})(\mu\text{-OOCCH}_3)]^+$ (**1**), which converts upon standing in acetonitrile solution into the green tetranuclear complex $[\text{Fe}_4(\text{N}_3\text{O}_2\text{-L})_4(\mu\text{-O})_2]^{4+}$ (**2**). A single-crystal X-ray structure analysis of $[\mathbf{2}][\text{PF}_6]_4 \cdot 5\text{MeCN}$ reveals **2** to contain four iron(III) centers, each of which is coordinated to three nitrogen atoms of a triazacyclononane ligand and is bridged by one oxo and two carboxylato bridges, a structural feature known from the active center of methane monooxygenase. Accordingly, complex **2** was found to catalyze the oxidative functionalization of methane with hydrogen peroxide in aqueous solution to give methanol, methyl hydroperoxide, and formic acid; the total turnover numbers attain 24 catalytic cycles within 4 h. To gain more insight into the catalytic process, the catalytic potential of **2** was also studied for the oxidation of higher alkanes, cycloalkanes, and isopropanol in acetonitrile, as well as in aqueous solution. The bond selectivities of the oxidation of linear and branched alkanes suggest a ferroxyl radical pathway.

Introduction

One of the most interesting reactions is without any doubt the catalytic hydroxylation of methane, performed by the enzyme methane monooxygenase (MMO), a non-heme diiron protein occurring in methanotrophic bacteria (see reviews¹ and recent original publications).² These microorganisms convert methane to methanol in a process coupled to the oxidation of the biological reducing agent NADH.



The reactive site in the enzyme has been identified by structural studies of soluble MMO extracted from *Methylococcus capsulatus* (Bath)³ and *Methylosinus trichosporium*

* To whom correspondence should be addressed. E-mail: georg.suess-fink@unine.ch.

[†] Université de Neuchâtel.

[‡] Russian Academy of Sciences.

- (1) (a) Wallar, B. J.; Lipscomb, J. D. *Chem. Rev.* **1996**, *96*, 2625–2658. (b) Shilov, A. E.; Shul'pin, G. B. *Chem. Rev.* **1997**, *97*, 2879–2932. (c) Shilov, A. E.; Shul'pin, G. B. *Activation and Catalytic Reactions of Saturated Hydrocarbons in the Presence of Metal Complexes*; Kluwer Academic Publishers: Dordrecht, The Netherlands, 2000; Chapter XI. (d) Baik, M.-H.; Newcomb, M.; Friesner, R. A.; Lippard, S. J. *Chem. Rev.* **2003**, *103*, 2385–2419. (e) Noodleman, L.; Lovell, T.; Han, W.-G.; Li, J.; Himo, F. *Chem. Rev.* **2004**, *104*, 459–508. (f) Yoshizawa, K. *Acc. Chem. Res.* **2006**, *39*, 375–382. (g) Zhang, J.; Zheng, H.; Groce, S. L.; Lipscomb, J. D. *J. Mol. Catal. A: Chem.* **2006**, *251*, 54–65. (h) Ragsdale, S. W. *Chem. Rev.* **2006**, *106*, 3317–3337. (i) Siegbahn, P. E. M.; Borowski, T. *Acc. Chem. Res.* **2006**, *39*, 729–738. (j) Sazinsky, M. H.; Lippard, S. J. *Acc. Chem. Res.* **2006**, *39*, 558–566.

- (2) (a) Baik, M.-H.; Gherman, B. F.; Friesner, R. A.; S. J. Lippard, *J. Am. Chem. Soc.* **2002**, *124*, 14608–14615. (b) Moe, L. A.; Hu, Z.; Deng, D.; Austin, R. N.; Groves, J. T.; Fox, B. G. *Biochemistry* **2004**, *43*, 15688–15701. (c) Gherman, B. F.; Baik, M.-H.; Lippard, S. J.; Friesner, R. A. *J. Am. Chem. Soc.* **2004**, *126*, 2978–2990. (d) Wei, P.; Skulan, A. J.; Mitia, N.; Yang, Y.-S.; Saleh, L.; Bollinger, J. M., Jr.; Solomon, E. I. *J. Am. Chem. Soc.* **2004**, *126*, 3777–3788. (e) Gherman, B. F.; Lippard, S. J.; Friesner, R. A. *J. Am. Chem. Soc.* **2005**, *127*, 1025–1037. (f) Sazinsky, M. H.; Lippard, S. J. *J. Am. Chem. Soc.* **2005**, *127*, 5814–5825. (g) Beauvais, L. G.; Lippard, S. J. *J. Am. Chem. Soc.* **2005**, *127*, 7370–7378. (h) Blazyk, J. L.; Gassner, G. T.; Lippard, S. J. *J. Am. Chem. Soc.* **2005**, *127*, 17364–17376. (i) Zheng, H.; Lipscomb, J. D. *Biochemistry* **2006**, *45*, 1685–1692. (j) Zhang, J.; Wallar, B. J.; Popescu, C. V.; Renner, D. B.; Thomas, D. D.; Lipscomb, J. D. *Biochemistry* **2006**, *45*, 2913–2926. (k) Murray, L. J.; Garcia-Serres, R.; Naik, S.; Huynh, B. H. Lippard, S. J. *J. Am. Chem. Soc.* **2006**, *128*, 7458–7459.
- (3) (a) Rosenzweig, A. C.; Frederick, C. A.; Lippard, S. J.; Nordlund, P. *Nature* **1993**, *366*, 537–543. (b) Rosenzweig, A. C.; Nordlund, P.; Takahara, P. M.; Frederick, C. A.; Lippard, S. J. *Chem. Biol.* **1995**, *2*, 409–418. (c) Whittington, D. A.; Lippard, S. J. *J. Am. Chem. Soc.* **2001**, *123*, 827–838.

OB3b⁴ to be a diiron center in the oxidized form containing a carboxylato and two hydroxo bridges.^{3c} Substantial progress has been made in understanding the key features of the catalytic hydroxylation on the basis of extensive experimental^{2,5} and theoretical studies.^{1,6} A few mechanisms have been proposed for the alkane oxidation with participation of MMO.^{1d} The crucial step of the methane-to-methanol conversion in the active site of soluble MMO can be attributed to the hydrogen atom abstraction from a methane molecule by a radical-like iron(IV) and iron(III) species.^{2a}

Soluble MMO from *M. capsulatus* (Bath) oxidizes normal pentane, hexane, and heptane to afford predominately (in the case of *n*-heptane even exclusively) 2-ols.^{7a} Scrambling of the stereochemistry was observed for *cis*-1,4-dimethylcyclohexane and *cis*-1,3-dimethylcyclohexane.^{7b} Iron complexes containing N and O ligands and carboxylato bridges can serve as models for hydroxylating enzyme centers (see reviews),⁸ with mononuclear⁹ and polynuclear¹⁰ examples being known. Biomimetic oxidation studies for alkane functionalization with iron complexes have been pioneered by R. H. Fish,¹¹ S. J. Lippard,¹² and L. Que, Jr.¹³ Hydrogen peroxide is usually used as an oxidant in alkane oxidations catalyzed by such complexes.¹⁴

Experimental Section

General. Solvents for catalytic experiments were of analytical grade (Acros, Merck or Cambridge Isotope Laboratories) and were used without distillation; they were only stored over molecular sieve

and under a nitrogen atmosphere. Solvents for synthesis were of technical grade and were purified by distillation under nitrogen and dried according to standard laboratory practices.¹⁵ Water was bidistilled and stored under nitrogen. Laboratory gases were

- (4) Elango, N.; Radhakrishnan, R.; Froland, W. A.; Wallar, B. J.; Earhart, C. A.; Lipscomb, J. D.; Ohlendorf, D. H. *Protein Sci.* **1997**, *6*, 556–568.
- (5) (a) Brazeau, B. J.; Lipscomb, J. D. *Biochemistry* **2000**, *39*, 13503–13515. (b) Brazeau, B. J.; Austin, R. N.; Tarr, C.; Groves, J. T.; Lipscomb, J. D. *J. Am. Chem. Soc.* **2001**, *123*, 11831–11837. (c) Brazeau, B. J.; Wallar, B. J.; Lipscomb, J. D. *J. Am. Chem. Soc.* **2001**, *123*, 10421–10422. (d) Jin, Y.; Lipscomb, J. D. *J. Biol. Inorg. Chem.* **2001**, *6*, 717–725. (e) Ambundo, E. A.; Friesner, R. A.; Lippard, S. J. *J. Am. Chem. Soc.* **2002**, *124*, 8770–8771.
- (6) (a) Siegbahn, P. E. M.; Blomberg, M. R. A. *Chem. Rev.* **2000**, *100*, 421–437. (b) Friesner, R. A.; Dunietz, B. D. *Acc. Chem. Res.* **2001**, *34*, 351–358. (c) Guallar, V.; Gherman, B. F.; Miller, W. H.; Lippard, S. J.; Friesner, R. A. *J. Am. Chem. Soc.* **2002**, *124*, 3377–3384. (d) Musaev, D. G.; Basch, H.; Morokuma, K. *J. Am. Chem. Soc.* **2002**, *124*, 4135–4148. (e) Torrent, M.; Vreven, T.; Musaev, D. G.; Morokuma, K.; Farkas, O.; Schlegel, H. B. *J. Am. Chem. Soc.* **2002**, *124*, 192–193. (f) Lovell, T.; Han, W.-G.; Liu, T.; Noodleman, L. *J. Am. Chem. Soc.* **2002**, *124*, 5890–5894.
- (7) (a) Green, J.; Dalton, H. *J. Biol. Chem.* **1989**, *264*, 17698–17703. (b) Leak, D. J.; Dalton, H. *Biocatalysis* **1987**, *1*, 23–36.
- (8) (a) *Biomimetic Oxidations Catalyzed by Transition Metal Complexes*; Meunier, B., Ed.; Imperial College: London, 2000. (b) Tschuva, E. Y.; Lippard, S. J. *Chem. Rev.* **2004**, *104*, 987–1012. (c) Kryatov, S. V.; Rybak-Akimova, E. V. *Chem. Rev.* **2005**, *105*, 2175–2226. (d) Punniyamurthy, T.; Velusamy, S.; Iqbal, J. *Chem. Rev.* **2005**, *105*, 2329–2363. (e) Tanase, S.; Bouwman, E. *Adv. Inorg. Chem.* **2006**, *58*, 29–75.
- (9) (a) Beck, A.; Barth, A.; Hübner, E.; Burzlaff, N. *Inorg. Chem.* **2003**, *42*, 7182–7188. (b) Ensing, B.; Buda, F.; Gribnau, M. C. M.; Baerends, E. J. *J. Am. Chem. Soc.* **2004**, *126*, 4355–4365. (c) Shul'pin, G. B.; Stoeckli-Evans, H.; Mandelli, D.; Kozlov, Y. N.; Vallina, A. T.; Woitiski, C. B.; Jimenez, R. S.; Carvalho, W. A. *J. Mol. Catal. A: Chem.* **2004**, *219*, 255–264. (d) Tanase, S.; Foltz, C.; de Gelder, R.; Hage, R.; Bouwman, E.; Reedijk, J. *J. Mol. Catal. A: Chem.* **2005**, *225*, 161–167. (e) Carvalho, N. M. F.; Horn, A., Jr.; Antunes, O. A. C. *Appl. Catal., A: General* **2006**, *305*, 140–145. (f) Tanase, S.; Gallego, P. M.; Bouwman, E.; Long, G. J.; Rebbouh, L.; Grandjean, F.; de Gelder, R.; Mutikainen, I.; Turpeinen, U.; Reedijk, J. *Dalton Trans.* **2006**, 1675–1684. (g) Britovsek, G. J. P.; England, J.; White, A. J. P. *Dalton Trans.* **2006**, 1399–1408. (h) Li, F.; Wang, M.; Ma, C.; Gao, A.; Chen, H.; Sun, L. *Dalton Trans.* **2006**, 2427–2434.
- (10) (a) Ménage, S.; Galey, J.-B.; Dumats, J.; Hussler, G.; Seité, M.; Luneau, I. G.; Chottard, G.; Fontecave, M. *J. Am. Chem. Soc.* **1998**, *120*, 13370–13382. (b) Mizuno, N.; Nozaki, C.; Kiyoto, I.; Misono, M. *J. Catal.* **1999**, *182*, 285–288. (c) Zheng, H.; Zang, Y.; Dong, Y.; Young, V. G.; Que, L., Jr. *J. Am. Chem. Soc.* **1999**, *121*, 2226–2235. (d) Mizuno, N. In *Polyoxalate Chemistry*; Pope, M., Mueller, A., Eds.; Kluwer: Dordrecht, The Netherlands, 2001; pp 335–345. (e) Tshuva, E. Y.; Lee, D.; Bu, W.; Lippard, S. J. *J. Am. Chem. Soc.* **2002**, *124*, 2416–2417. (f) Lee, D.; Lippard, S. J. *Inorg. Chem.* **2002**, *41*, 827–837. (g) Lee, D.; Lippard, S. J. *Inorg. Chem.* **2002**, *41*, 2704–2719. (h) Nizova, G. V.; Krebs, B.; Süß-Fink, G.; Schindler, S.; Westerheide, L.; Gonzalez Cuervo, L.; Shul'pin, G. B. *Tetrahedron* **2002**, *58*, 9231–9237. (i) Costas, M.; Cady, C. W.; Kryatov, S. V.; Ray, M.; Ryan, M. J.; Rybak-Akimova, E. V.; Que, L., Jr. *Inorg. Chem.* **2003**, *42*, 5519–5530. (j) Yoon, S.; Lippard, S. J. *J. Am. Chem. Soc.* **2004**, *126*, 16692–16693. (k) Kryatov, S. V.; Chavez, F. A.; Reynolds, A. M.; Rybak-Akimova, E. V.; Que, L., Jr.; Tolman, W. B. *Inorg. Chem.* **2004**, *43*, 2141–2150. (l) Moreira, R. F.; Tshuva, E. Y.; Lippard, S. J. *Inorg. Chem.* **2004**, *43*, 4427–4434. (m) Boskovic, C.; Sieber, A.; Chaboussant, G.; Güdel, H. U.; Ensling, J.; Wernsdorfer, W.; Neels, A.; Labat, G.; Stoeckli-Evans, H.; Janssen, S. *Inorg. Chem.* **2004**, *43*, 5053–5068. (n) Mortensen, M. N.; Jensen, B.; Hazell, A.; Bond, A. D.; McKenzie, C. J. *Dalton Trans.* **2004**, 3396–3402. (o) Shul'pin, G. B.; Nizova, G. V.; Kozlov, Y. N.; Gonzalez Cuervo, L.; Süß-Fink, G. *Adv. Synth. Catal.* **2004**, *346*, 317–332. (p) Yoon, S.; Lippard, S. J. *J. Am. Chem. Soc.* **2005**, *127*, 8386–8397. (q) Kodera, M.; Itoh, M.; Kano, K.; Funabiki, T.; Reglier, M. *Angew. Chem., Int. Ed.* **2005**, *44*, 7104–7106. (r) Trettenhahn, G.; Nagl, M.; Neuwirth, N.; Arion, V. B.; Jary, W.; Pöchlauer, P.; Schmid, W. *Angew. Chem., Int. Ed.* **2006**, *45*, 2794–2798. (s) Gutkina, E. A.; Trukhan, V. M.; Pierpont, C. G.; Mkoyan, S.; Strelets, V. V.; Nordlander, E.; Shtenman, A. A. *Dalton Trans.* **2006**, 492–501. (t) Carson, E. C.; Lippard, S. J. *Inorg. Chem.* **2006**, *45*, 828–836. (u) Carson, E. C.; Lippard, S. J. *Inorg. Chem.* **2006**, *45*, 837–848. (v) Yoon, S.; Lippard, S. J. *Inorg. Chem.* **2006**, *45*, 5438–5446. (w) Zhao, M.; Song, D.; Lippard, S. J. *Inorg. Chem.* **2006**, *45*, 6323–6330. (x) Bonchio, M.; Carraro, M.; Sartorel, A.; Scorrano, G.; Kortz, U. *J. Mol. Catal. A: Chem.* **2006**, *251*, 93–99. (y) Botar, B.; Geletii, Y. V.; Kögerler, P.; Musaev, D. G.; Morokuma, K.; Weinstock, I. A.; Hill, C. L. *J. Am. Chem. Soc.* **2006**, *128*, 11268–11277.
- (11) (a) Vincent, J. B.; Huffman, J. C.; Christou, G.; Li, Q.; Nanny, M. A.; Hendrickson, D. N.; Fong, R. H.; Fish, R. H. *J. Am. Chem. Soc.* **1988**, *110*, 6898–6900. (b) Fish, R. H.; Konings, M. S.; Oberhausen, K. J.; Fong, R. H.; Yu, W. M.; Christou, G.; Vincent, J. B.; Coggin, D. A. K.; Buchanan, R. M. *Inorg. Chem.* **1991**, *30*, 3002–3006. (c) Buchanan, R. M.; Chen, S.; Richardson, J. F.; Bressan, M.; Forti, L.; Morvillo, A.; Fish, R. H. *Inorg. Chem.* **1994**, *33*, 3208–3209. (d) Rabion, A.; Chen, S.; Wang, J.; Buchanan, R. M.; Seris, J.-L.; Fish, R. H. *J. Am. Chem. Soc.* **1995**, *117*, 12356–12357. (e) Rabion, A.; Buchanan, R. M.; Seris, J.-L.; Fish, R. H. *J. Mol. Catal. A: Chem.* **1997**, *116*, 43–47. (f) Neimann, K.; Neumann, R.; Rabion, A.; Buchanan, R. M.; Fish, R. H. *Inorg. Chem.* **1999**, *38*, 3575–3580.
- (12) (a) Armstrong, W. H.; Lippard, S. J. *J. Am. Chem. Soc.* **1983**, *105*, 4837–4838. (b) Gorun, S. M.; Lippard, S. J. *Nature* **1986**, *319*, 666–668. (c) Hartman, J. A. R.; Rardin, R. L.; Chaudhuri, P.; Pohl, K.; Wiegand, K.; Nuber, B.; Weiss, J.; Papaefthymiou, G. C.; Frankel, R. B.; Lippard, S. J. *J. Am. Chem. Soc.* **1987**, *109*, 7387–7396.
- (13) (a) Lauffer, R. B.; Heistand, R. H., II; Que, L., Jr. *J. Am. Chem. Soc.* **1981**, *103*, 3947–3949. (b) Pyrz, J. W.; Roe, A. L.; Stern, L. J.; Que, L., Jr. *J. Am. Chem. Soc.* **1985**, *107*, 614–620. (c) Borovik, A. S.; Que, L., Jr. *J. Am. Chem. Soc.* **1988**, *110*, 2345–2347. (d) Yan, S.; Cox, D. D.; Pearce, L. L.; Juarez-Garcia, C.; Que, L., Jr.; Zhang, J. H.; O'Connor, C. J. *Inorg. Chem.* **1989**, *28*, 2507–2509. (e) Norman, R. E.; Yan, S.; Que, L., Jr.; Backes, G.; Ling, J.; Sanders-Loehr, J.; Zhang, J. H.; O'Connor, C. J. *J. Am. Chem. Soc.* **1990**, *112*, 1554–1562. (f) Leising, R. A.; Norman, R. E.; Que, L., Jr. *Inorg. Chem.* **1990**, *29*, 2553–2555. (g) Costas, M.; Chen, K.; Que, L. *Coord. Chem. Rev.* **2000**, *200*, 517–544.
- (14) Shul'pin, G. B. Oxidations of C–H Compounds Catalyzed by Metal Complexes. In *Transition Metals for Organic Synthesis*, 2nd ed.; Beller, M., Bolm, C., Eds.; Wiley-VCH: Weinheim, Germany, 2004; Vol 2, Chapter 2.2, pp 215–242.
- (15) Perrin, D. D.; Armarego, W. L. F. *Purification of Laboratory Chemicals*; Pergamon Press: Oxford, U.K., 1998.

purchased from Carbagas and used directly from the cylinders without further purification.

The macrocyclic ligand precursor 1,4-dimethyl-1,4,7-triazacyclononane was synthesized and purified according to the published method.¹⁶ All other commercial compounds were of analytical grade and were used as received (Acros, Aldrich, and Fluka). Hydrogen peroxide was used as a solution in water (30%, not stabilized, Fluka) and stored at 4 °C. The exact concentration was determined using potassium permanganate titration and by UV spectroscopy (230 nm, $\epsilon = 81 \text{ M}^{-1} \text{ cm}^{-1}$). Hydrobromic acid was used as a solution in glacial acetic acid (33%, Riedel de Haën).

Instrumentation and Analyses. All syntheses were carried out by standard Schlenk techniques under a nitrogen or argon atmosphere unless stated otherwise. Silica (60 Å, 63–200 mesh) for column chromatography was purchased from Chemie Brunschwig AG. UV–vis spectra were recorded using an UVICON-930 spectrophotometer; the samples were placed in quartz 2 mm or 10 mm high-precision cells with an appropriate solvent used as reference. Microsoft Excel was used for data analysis. Infrared spectra were recorded with a Perkin-Elmer Spectrum One spectrometer in transmission mode where the absorptions are given in reciprocal centimeters (cm^{-1}). Intensity data are described with the following abbreviations: vs = very strong, s = strong, m = medium, w = weak, sh = shoulder. Nuclear magnetic resonance spectra were recorded using a Bruker AMX 400. ^1H and ^{13}C { ^1H -decoupled} NMR used the solvent as the internal standard. ESI mass spectra were measured by the Analytical Service of the University of Neuchâtel (Switzerland) using a LCQ Finnigan spectrometer. Microanalyses were carried out by the Laboratory of Pharmaceutical Chemistry, University of Geneva (Switzerland).

Crystallographic Analysis. Crystal data for $[\text{2}][\text{PF}_6]_4 \cdot 5 \text{ MeCN}$: $\text{C}_{50}\text{H}_{95}\text{F}_{24}\text{Fe}_4\text{N}_{17}\text{O}_{10}\text{P}_4$, $M = 1897.71$, monoclinic, space group $P2_1/c$ (No. 14), $a = 22.673(2) \text{ \AA}$, $b = 14.8307(8) \text{ \AA}$, $c = 23.388(2) \text{ \AA}$, $\beta = 99.387(10)^\circ$, $V = 7758.9(10) \text{ \AA}^3$, $T = 173(2) \text{ K}$, $Z = 4$, $D_c = 1.625 \text{ g cm}^{-3}$, 15 205 reflections measured, 4675 unique ($R_{\text{int}} = 0.1477$) which were used in all calculations. The crystal was mounted on a Stoe Image Plate Diffraction system equipped with a ϕ circle goniometer, using Mo $K\alpha$ graphite-monochromated radiation ($\lambda = 0.71073 \text{ \AA}$) with ϕ range of 0–200°, an increment of 1.0°, a 2θ range of 2.0–26°, and $D_{\text{max}} - D_{\text{min}} = 12.45 - 0.81 \text{ \AA}$. The structure was solved by direct methods using the program SHELXS-97.¹⁷ The refinement and all further calculations were carried out using SHELXL-97,¹⁸ with 941 parameters: $R1 = 0.0701$ ($I > 2\sigma(I)$), $wR2 = 0.2037$, $\text{GOF} = 0.745$, and the max/min residual density = $0.972/-0.755 \text{ e\AA}^{-3}$. The H-atoms were included in calculated positions and treated as riding atoms using the SHELXL default parameters. A semiempirical absorption correction was applied using DIFABS (PLATON03,¹⁹ $T_{\text{min}} = 0.346$, $T_{\text{max}} = 0.767$). Molecular structure representations were drawn with ORTEP,²⁰ MERCURY,²¹ and POV-RAY.²²

Gas Chromatography. GC-analyses were performed on a Dani 86.10 gas chromatograph equipped with a split-mode capillary

injection system and flame ionization detector using a CP-WAX52CB capillary column (25 m \times 0.32 mm \times 0.25 μm), integrator SP-4400, and helium as carrier gas. Acetonitrile or nitromethane was used as internal standards. The flame ionization detector response factors were obtained after calibration experiments, using a standard substrate mixtures. Gaseous mixtures (O_2 , N_2 , CH_4 , CO and CO_2) were quantified after injection of 500 μL with a gastight syringe on a packed column (Carboxen-1000 60/80, 4.5 m \times 3.1 mm, Supelco) using a thermal conductivity detector (TCD).

Catalytic Experiments. Oxidation of Methane. The experiments using methane as substrate and synthetic air as oxidant were carried out in 100 mL autoclaves equipped with glass-lined steel vessels containing a magnetic bar. In a typical experiment, the glass tube containing the solvent, catalyst, cocatalyst, and hydrogen peroxide was introduced in the steel vessel of the autoclave, which was closed hermetically and purged with air. After that, the autoclave was pressurized with air and with methane, in this order, to the corresponding pressures and heated to the corresponding temperature under vigorous stirring. **CAUTION!** *The combination of air or molecular oxygen and H_2O_2 with organic compounds at elevated pressures and temperatures may be explosive!* After the indicated reaction time, the autoclave was cooled in ice, and the pressure was released; the samples of gaseous mixture were taken in a 200 mL reservoir and analyzed by GC. Two aliquots of the reaction mixture were taken for ^1H NMR and for GC analysis using MeCN as internal standard.

Oxidation of Higher Alkanes. The oxidation of higher alkanes was carried out in thermostated cylindrical vessels connected to a reflux tube; when the reaction temperature was higher than 40 °C, the vessel was opened to air. In a typical experiment, a portion of hydrogen peroxide was added to the solution of the catalyst and substrate in acetonitrile. After certain time intervals, samples (0.6 mL) were taken. The samples were analyzed twice: before and after addition of triphenylphosphine to reduce the remaining hydrogen peroxide to water and the alkyl hydroperoxide to the corresponding alcohol;²³ the reaction is complete after 15 min. Each sample was injected in the GC twice, 0.2 μL each time. The comparison of the concentrations of cyclohexanone and cyclohexanol before and after reduction allows us to estimate the real concentrations of cyclohexyl hydroperoxide, cyclohexanone, and cyclohexanol present in the reaction mixture.²³

Oxidation of *i*-Propanol. The oxidation of *i*-propanol was carried out in air in thermostated cylindrical Pyrex vessels with vigorous stirring. The total volume of the reaction solution was 10 mL. In a typical experiment, hydrogen peroxide (30% aqueous solution, 0.50 M) was added to a mixture containing the catalyst, cocatalyst, and substrate in water or in acetonitrile. Blank experiments were carried out without catalyst. The samples of the reaction solution were analyzed by GC.

Syntheses. Sodium 2-(4,7-dimethyl-1,4,7-triazacyclononan-1-yl)acetate (Na[L]). In a 100 mL Schlenk tube, 3.14 g (20.0 mmol) of freshly distilled 1,4-dimethyl-1,4,7-triazacyclononane was dissolved in 10 mL of water at room temperature, and an aqueous solution of sodium bromoacetate (20 mmol, 10 mL), prepared by neutralization of 2.78 g (20 mmol) of bromoacetic acid with 0.80

- (16) Flassbeck, C.; Wieghardt, K. *Z. Anorg. Allg. Chem.* **1992**, *608*, 60–68.
 (17) Sheldrick, G. M. *SHELXS-97, Program for Crystal Structure Solution*; University of Göttingen: Göttingen, Germany, 1997.
 (18) Sheldrick, G. M. *SHELXL-97, Program for Crystal Structure Refinement*; University of Göttingen: Göttingen, Germany, 1997.
 (19) Spek, A. L. *J. Appl. Cryst.* **2003**, *36*, 7–13.
 (20) Farrugia, L. J. *J. Appl. Cryst.* **1997**, *30*, 565.
 (21) Bruno, I. J.; Cole, J. C.; Edgington, P. R.; Kessler, M.; Macrae, C. F.; McCabe, P.; Pearson, J.; Taylor, R. *Acta Crystallogr.* **2002**, *B58*, 389–397.
 (22) Fenn, T. D.; Ringe, D.; Petsko, G. A. *J. Appl. Crystallogr.* **2003**, *36*, 944–947.

- (23) (a) Shul'pin, G. B. *J. Mol. Catal. A: Chem.* **2002**, *189*, 39–66. (b) Shul'pin, G. B. *C. R. Chim.* **2003**, *6*, 163–178. (c) Shul'pin, G. B.; Druzhinina, A. N. *React. Kinet. Catal. Lett.* **1992**, *47*, 207–211. (d) Shul'pin, G. B.; Nizova, G. V. *React. Kinet. Catal. Lett.* **1992**, *48*, 333–338. (e) Shul'pin, G. B.; Attanasio, D.; Suber, L. *J. Catal.* **1993**, *142*, 147–152. (f) Shul'pin, G. B.; Nizova, G. V.; Kozlov, Y. N. *New J. Chem.* **1996**, *20*, 1243–1256.

Tetrairon Complex $[Fe_4(N_3O_2-L)_4(\mu-O)_2]^{4+}$

g (20 mmol) NaOH, was added dropwise (5 min). The temperature was raised to 80 °C, and 1.00 g (25 mmol) of NaOH dissolved in 5 mL of water was added dropwise (5 min). The temperature was maintained at 80 °C for 2 h, until the reaction was complete. The light-yellow solution was evaporated (0.05 mbar, 50 °C), and the solid product was extracted with CH_2Cl_2 (3 × 50 mL), dried over anhydrous Na_2SO_4 , and filtered under a nitrogen atmosphere. A white-yellowish hygroscopic powder was obtained after solvent evaporation and drying in vacuo (0.01 mbar, 50 °C, 48 h).

Na[L]. Yield: 70–83%. 1H NMR (400 MHz, $CDCl_3$): δ 3.10 (s, 2H, NCH_2COONa), 2.55–2.48 (m, 12H, NCH_2CH_2N) and 2.33 (s, 6H, NCH_3). ^{13}C NMR { 1H decoupled} (100 MHz, $CDCl_3$): δ 177.2 (NCH_2COONa), 63.7 (NCH_2COONa), 55.0, 54.8, 53.2 (3 × NCH_2CH_2N) and 45.9 (NCH_3). MS (ESI negative mode, acetone): m/z 215 ($[L]^-$). IR (KBr pellets) ν (cm^{-1}): 3418 (s), 2945 (s), 2853 (s), 2792 (s), 1594 (s), 1454 (s), 1405 (s), 1367 (s), 1078 (m), 1036 (s), 830 (m), 748 (m) and 612 (m). Anal. Calcd for $C_{10}H_{20}N_3O_2 \cdot Na \cdot 1.5 CH_2Cl_2$: C, 37.88; H, 6.36; N, 11.52. Found: C, 38.07; H, 6.50; N, 11.52%.

General procedure for $[L_2Fe_2(O)(OOCMe)][PF_6]$ ([1]**)[PF_6] and $[L_4Fe_4(O)_2][PF_6]_4$ (**[2]**)[PF_6]₄.** In a 50 mL Schlenk tube, a mixture of $Na[L] \cdot 1.5CH_2Cl_2$ (364 mg, 1.00 mmol), $FeSO_4 \cdot 7H_2O$ (278 mg, 1.00 mmol), and KPF_6 (276 mg, 1.50 mmol) in aqueous ethanol (60%, 8 mL) was stirred under an argon atmosphere at room temperature for 2 h. The resulting dark green solution (pH 3.8–4.2) was cooled to 0 °C, before 2 mL of a freshly prepared aqueous solution containing H_2O_2 (100 μ L, 1.00 mmol) and NaOH (48 mg, 1.20 mmol) was added. The brown-green mixture was stirred in air at 20 °C for 2 h (pH 4.5), before celite (basic, pH 9) was added. After filtration the product was extracted from the celite bed by being washed two times with 5 mL of acetonitrile, and the combined washings were evaporated in vacuo (0.05 mbar, 20 °C, 2h). The green-brown residue was dissolved in acetonitrile, and after standing for a week (TLC testing), two products were separated by column chromatography on silica (eluent MeCN/MeOH 5:1–2:1). The yield of the green product varied from 5 to 15% depending on dilution, as well as on time. The green fraction containing **[2]**– $[PF_6]_4$ was evaporated, washed four times with 10 mL of ethanol, and dried in vacuo. Single crystals of **[2]**– $[PF_6]_4 \cdot 5MeCN$ suitable for X-ray analysis were grown from an acetonitrile solution into which the ether was allowed to slowly diffuse within 72 h. The brown-orange fraction containing **[1]**– $[PF_6]$ was evaporated, extracted in acetone, and crystallized with ether. A microcrystalline powder was obtained within 48 h.

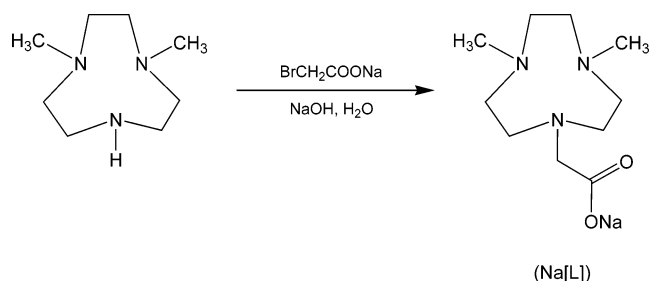
$[L_2Fe_2(O)(OOCMe)][PF_6]$ ([1]**)[PF_6].** Yield: 28–40%. 1H NMR (400 MHz, CD_3CN): δ 35.5, 31.5 (br, 4H, NCH_2COO), 28–18 (br, 28H, NCH_2CH_2N , NCH_3), 15.2 (br, 4H, $NCHHCH_2N$), 11.5 (br, 3H, $OOCCH_3$) and 8.1 (br, 4H, $NCHHCH_2N$). MS (ESI, positive mode, MeCN): m/z 634 (70%, $[1 + H + H_2O]^{2+}$), 651 (10%, $[1]^+$), 615 (10%, $^{1+}$), 416 (10%, $[LFe + PF_6]^+$). UV–vis (CH_3CN) λ_{max} (ϵ): 663 (160), 503 (1040), 449 (1600), 421 (1800), 326 cm^{-1} (15 500 $M^{-1} cm^{-1}$). IR (KBr pellets) ν (cm^{-1}): 3435 (s), 2930 (m), 1643 (s), 1578 (s), 1466 (s), 1384 (s), 1357 (s), 1103 (m), 1024 (m), 842 (vs), 781 (s), 740 (m), 559 (s). Anal. Calcd for $C_{22}H_{44}Fe_2N_6O_7PF_6 \cdot 2KPF_6$: C, 23.40; H, 3.93; N, 7.44. Found: C, 23.22; H, 3.80; N, 7.25%.

$[L_4Fe_4(O)_2][PF_6]_4$ ([2]**)[PF_6]₄.** Yield: 5–15%. MS (ESI, positive mode, acetone): m/z 575 ($[L_2Fe_2(O) + H + H_2O]^{3+}$). UV–vis (CH_3CN) λ_{max} (ϵ): 578 (300), 501 (670), 491 (710), 325 cm^{-1} (24 500 $M^{-1} cm^{-1}$). IR (KBr pellets) ν (cm^{-1}): 2925 (m), 1622 (vs), 1568 (m), 1407 (s), 1384 (m), 1304 (m), 1079 (m), 1023 (m), 841 (vs), 773 (s), 753 (s) and 559 (s). Anal. Calcd for $C_{40}H_{84}$ –

$Fe_4N_{12}O_{10}P_4F_{24}$: C, 28.32; H, 4.99; N, 9.91. Found: C, 28.73; H, 4.67; N, 10.32%.

Results and Discussion

Ligand and Complex Syntheses. The ligand L containing a pendent acetato arm is accessible by reaction of the 1,4-dimethyl-1,4,7-triazacyclononane with sodium bromoacetate, adapting a procedure previously described for 1,4,7-triazacyclononane-1,4,7-triacetate.²⁴ In contrast to the triacetate derivative, L can be successfully isolated from the alkaline aqueous solution by extraction with dichloromethane in the form of the sodium salt. The new ligand is fully characterized by MS and NMR spectroscopy, as well as by satisfactory element analytical data.



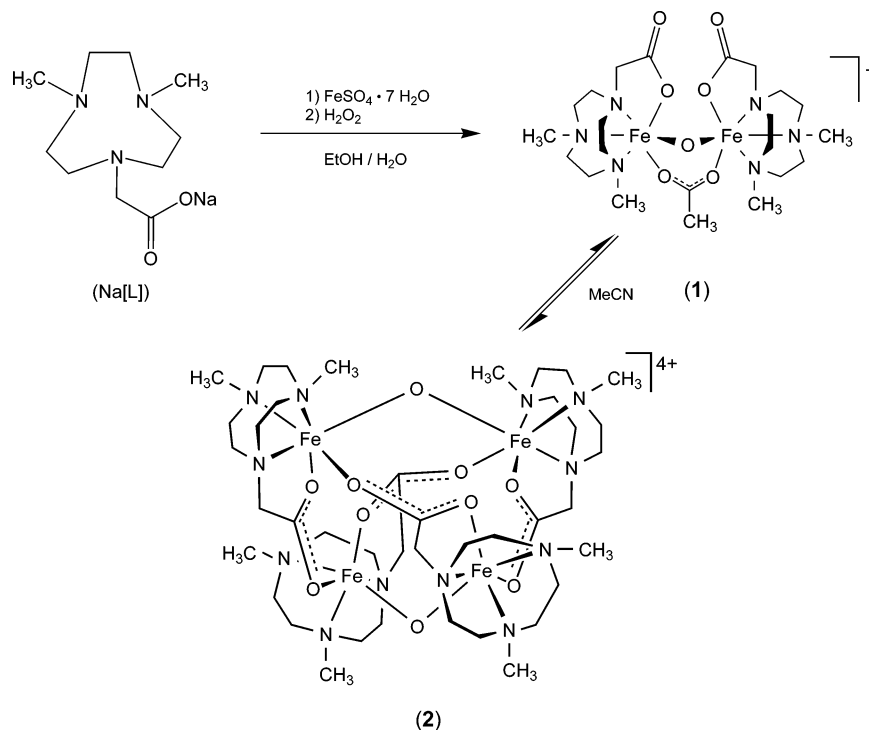
Iron(II) sulfate heptahydrate reacts readily with Na[L] in moist ethanol, and after the subsequent oxidation with hydrogen peroxide, a brownish product can be extracted with acetonitrile. Immediate workup shows the acetonitrile solution to contain a dinuclear iron(III) complex, considered to be $[L_2Fe_2(O)(OOCMe)]^+$ (**1**) on the basis of the spectroscopic and element-analytical characterization of the hexafluorophosphate salt. Upon standing at room temperature in acetonitrile over several days, two cationic iron(III) complexes are observed in solution, which can be separated by column chromatography and isolated as the hexafluorophosphate salts. The brown fraction contains **1**, while the green fraction shows a tetranuclear iron(III) complex $[L_4Fe_4(O)_2]^{4+}$ (**2**), see Scheme 1. An analogous interconversion of a dinuclear iron(III) into a tetranuclear iron(III) complex is reported with tetradentate ethylenediamine diacetate^{10a} and pyridyl-amino carboxylato ligands.²⁵

Green X-ray quality crystals of **[2]**– $[PF_6]_4 \cdot 5MeCN$ are obtained by slow diffusion of ether into an acetonitrile solution containing **[2]**– $[PF_6]_4$. A microcrystalline brown-orange powder of **[1]**– $[PF_6] \cdot 2KPF_6$ was obtained by slow diffusion of ether into an acetone solution containing **1** and KPF_6 .

The brown microcrystalline product, **[1]**– $[PF_6] \cdot 2KPF_6$, is considered to be $[(N_3O-L)_2Fe_2(\mu-O)(\mu-OOCMe)][PF_6] \cdot 2KPF_6$ on the basis of the analytical and spectroscopic data, by analogy to the known compound $[(cmtacn)_2Fe_2(\mu-O)(\mu-OOCMe)][ClO_4] \cdot NaClO_4 \cdot 2H_2O$ ($cmtacn = 1$ -carboxymethyl-1,4,7-triazacyclononane), containing the non-methylated

- (24) (a) Wieghardt, K.; Bossek, U.; Chaudhuri, P.; Herrmann, W.; Menke, B. C.; Weiss, J. *Inorg. Chem.* **1982**, *21*, 4308–4314. (b) De Vos, D. E.; Bein, T. *J. Organomet. Chem.* **1996**, *520*, 195–200.
(25) (a) Nishino, S.; Takahashi, Y.; Nishida, Y. *Inorg. Chem. Commun.* **2002**, *5*, 609–611. (b) Mortensen, M. N.; Jensen, B.; Hazell, A.; Bond, A. D.; McKenzie, C. *J. Dalton Trans.* **2004**, 3396–3402.

Scheme 1. Reaction of Sodium 2-(4,7-Dimethyl-1,4,7-triazacyclononan-1-yl) Acetate (Na[L]) with Iron(II) Sulfate Heptahydrate in the Presence of Hydrogen Peroxide



ligand instead of L, for which the molecular structure is known by single-crystal X-ray analysis.²⁶

The presence of an acetato bridge in **1** is surprising, since in the reaction of $\text{FeSO}_4 \cdot 7 \text{H}_2\text{O}$ with L in aqueous ethanol, which yields **1** and **2**, no acetate is added. However, we found that, upon addition of hydrogen peroxide to the aqueous ethanol solution of Fe^{2+}/L , followed by stirring in air for 2 h at room temperature, a significant quantity of acetic acid is formed (detected after acidification and GC analysis), which apparently originates from the iron-catalyzed oxidation of ethanol.

The ^1H NMR spectrum of **1** in CD_3CN is shown in Figure 1. The NMR spectra of paramagnetic dinuclear $\text{Fe(III)}-\text{Fe(III)}$ complexes containing 1,4,7-triazacyclononane (tacn) and 1,4,7-trimethyl-1,4,7-triazacyclononane (tmtacn) ligands, as well as acetato and oxo bridges, have been reported and interpreted using labeling experiments.²⁷ The strong coupling

between the iron(III) centers causes the smaller range of chemical shifts (from 0 to +35 ppm), as compared to the analogous $\text{Mn(III)}-\text{Mn(III)}$ complexes (from -160 to +120 ppm).

The sharp resonance at 11.5 ppm (b) corresponds to the methyl group of the bridging μ -acetato ligand and compares well to the 11.4 ppm value reported for those in $[(\text{tmtacn})_2\text{Fe}_2(\text{O})(\text{OOCMe})_2]^{2+}$ and $[(\text{tacn})_2\text{Fe}_2(\text{O})(\text{OOCMe})_2]^{2+}$.²⁷ Since three $\text{N}-\text{CH}_3$ moieties of the macrocycle ligand in $[(\text{tmtacn})_2\text{Fe}_2(\text{O})(\text{OOCMe})_2]^{2+}$ are not equivalent, one of the methyl groups that is trans coordinated with respect to the oxo bridge gives rise to the upfield signal around 14.8 ppm.²⁷ We assign the resonance around 15.2 ppm in the spectrum of **1** to four “axial” methylene protons (c) near the nitrogen atoms trans-coordinated to the oxo bridge, which are more deshielded than the four “equatorial” methylene protons (a) with δ 8.1 ppm. This assumption is consistent with the relative intensities of these resonances, as well with the literature data^{27,28} and X-ray analyses of $[\mathbf{2}][\text{PF}_6]_4 \cdot 5\text{MeCN}$ and $[(\text{cmtacn})_2\text{Fe}_2(\mu\text{-O})(\mu\text{-OOCMe})][\text{ClO}_4] \cdot \text{NaClO}_4 \cdot 2 \text{H}_2\text{O}$.²⁶ Two broad resonances centered around 31.5 and 35.5 ppm can be attributed to the equatorial (e) and axial (f) methylene protons of the pendent acetato arms, the axial ones being more deshielded and expected to be shifted to downfield values. Because of the significant overlap between the signals from 18 to 28 ppm (d), the detailed assignment is problematic, but the N-methyl protons (nonequivalent, near 22 ppm), as well as

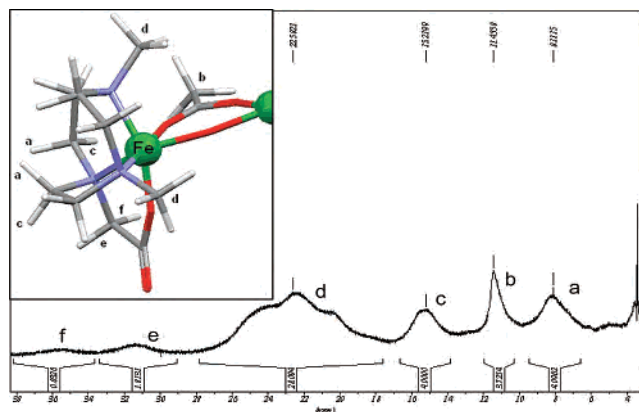


Figure 1. ^1H NMR (400 MHz) spectrum of the paramagnetic complex $[\text{L}_2\text{Fe}_2(\text{O})(\text{OOCMe})][\text{PF}_6]$ ($[\mathbf{1}][\text{PF}_6]$) measured in CD_3CN at 27 °C.

(26) Graham, B.; Moubaraki, B.; Murray, K. S.; Spiccia, L.; Cashion, J. D.; Hockless, D. C. R. *J. Chem. Soc., Dalton Trans.* **1997**, 5, 887–893.

(27) Hage, R.; Gunnewegh, E. A.; Niël, J.; Tjan, F. S. B.; Weyhermüller, T.; Wieghardt, K. *Inorg. Chim. Acta* **1998**, 268, 43–48.

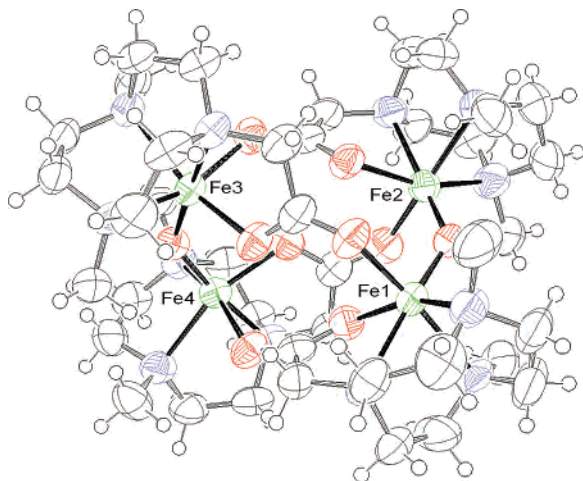


Figure 2. Molecular structure of $[L_4Fe_4(O)_2]^{4+}$ (**2**) in $[2][PF_6]_4 \cdot 5MeCN$; displacement ellipsoids are drawn at the 50% probability level. The MeCN and hexafluorophosphate molecules are omitted for clarity.

the other methylene protons in the L ligand, can be assigned to the signal d.

The ESI-MS spectrum of **1** in acetonitrile shows the parent peak at m/z 634 (70%, $[1 + H + H_2O]^{2+}$) and minor peaks at m/z 651 (10%, $[1]^+$), 615 (10%, $^{1+}$), and 416 (10%, $[LFe + PF_6]^+$). Absorptions at 781 and 740 cm^{-1} , observed in the infrared spectrum, can be assigned to the asymmetric Fe–O–Fe stretch modes, shifted to higher values than those in dinuclear complexes $[(dmtacn)_2Fe_2(O)(OOCMe)_2]^{2+}$ (725 cm^{-1}) and $[(dmtacn)_2Fe_2(O)(OOCPh)_2]^{2+}$ (724 cm^{-1}) ($dmtacn = 1,4$ -dimethyl-1,4,7-triazacyclononane)²⁹ but comparable to those in **2**. Since the vibration energies are indicative of the Fe–O–Fe angle parameters, we can assume that in **1** the Fe–O–Fe angle falls in the range from 130 to 135° (129° in $[(cmtacn)_2Fe_2(O)(OOCMe)]^+$ and 136° in **2**). The $\nu_{as}(C-O)$ stretching frequency of the bridging acetato in **1** is observed at 1578 cm^{-1} ; $\nu_s(C-O)$ frequency appears at 1466 cm^{-1} , while the bands at 1646 and 1359 cm^{-1} are from the monodentate pendent carboxyl groups of the ligand. These bands are shifted by 10–30 cm^{-1} to higher values than those in $[(cmtacn)_2Fe_2(O)(OOCMe)]^+$,²⁶ which could indicate incorporation of voluminous KPF_6 ion pairs between two acetato pendent arms. The UV–vis spectra of **1** and $[(cmtacn)_2Fe_2(O)(OOCMe)]^+$ are very similar;²⁶ in acetonitrile, both complexes show absorption maxima around λ (ϵ , for **1**, $M^{-1} cm^{-1}$) 663 (160), 503 (1040), 449 (1600), 421 (1800), and 326 (15500). The elemental analysis of $[1][PF_6] \cdot 2KPF_6$ gives 23.22 (C), 3.80 (H), and 7.25% (N), compared to the calculated values of 23.40, 3.93, and 7.44% respectively.

A single-crystal X-ray structure analysis of $[2][PF_6]_4 \cdot 5MeCN$ reveals **2** to contain four iron(III) centers (Figures 2 and 3), each of which is coordinated to three nitrogen atoms of a triazacyclononane ligand and bridged by one oxo and two carboxylato bridges, a structural feature known from the active center of methane monooxygenase.^{1,3} The tetrairon

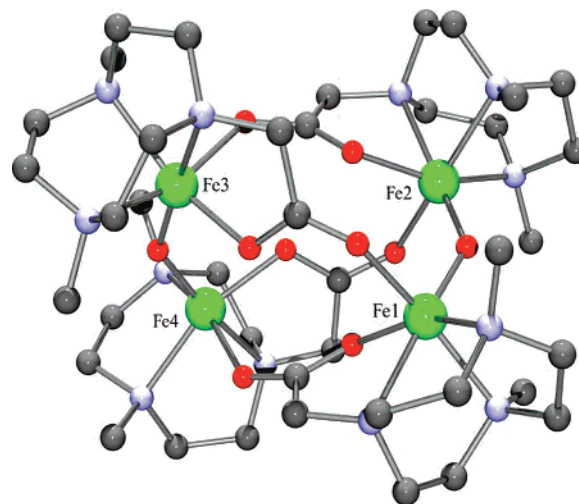


Figure 3. Simplified structural picture of **2** showing coordination mode of the four iron(III) centers in $[2][PF_6]_4 \cdot 5MeCN$; hydrogen atoms, MeCN, and hexafluorophosphate molecules are omitted for clarity.

Table 1. Selected Bond Lengths (Å) and Angles (deg) for $[2][PF_6]_4 \cdot 5MeCN$

	Fe(1)	Fe(2)	Fe(3)	Fe(4)
Fe–Fe (through oxo)	3.347(2)	3.347(2)	3.328(2)	3.328(2)
Fe–Fe (through acetato)	5.334(2)	5.330(2)	5.334(2)	5.337(2)
Fe–O (oxo)	1.803(5)	1.803(6)	1.805(5)	1.791(5)
Fe–O (own acetato)	1.997(5)	1.997(6)	2.002(5)	1.991(5)
Fe–O (bridged acetato)	2.092(6)	2.071(6)	2.064(6)	2.086(6)
Fe–N (acetato-substituted)	2.269(6)	2.271(7)	2.257(6)	2.250(6)
Fe–N (Me)	2.179(7)	2.175(7)	2.189(6)	2.197(7)
Fe–N (Me)	2.207(6)	2.208(7)	2.211(6)	2.204(6)
Fe–O–Fe (oxo)	136.2(8)	136.2(8)	135.4(5)	135.4(5)
O–C–O (own acetato arm)	122.7(5)	123.8(7)	123.9(9)	122.7(1)

core represents a tetrahedron with two short edges (μ -oxo-bridges) and four long ones (μ -carboxylato-bridges). The Fe–Fe distances of the oxo-bridged iron(III) centers are 3.328(2) and 3.347(2) Å, which are longer than those in the dinuclear Fe(III)–Fe(III) cations $[(dmtacn)_2Fe_2(O)(OOCMe)_2]^{2+}$ (3.104(1) Å) and $[(tmtacn)_2Fe_2(O)(OOCMe)_2]^{2+}$ (3.12(4) Å)^{12c} but compare well to those in the tetrairon dioxo complex $[Fe_4(bedda)_4(O)_2]$ (3.389(4) Å)^{10a} ($bedda = N,N'$ -bis(3,4,5-trimethoxybenzyl)-ethylenediamine N,N' -diacetate). The Fe–N (acetato-substituted) bonds are always in trans coordination to the oxo bridge, and they are slightly longer than those trans to the acetato bridges because of the greater trans influence of the oxo bridge. Furthermore, in **2**, the Fe–O–Fe angles of the μ -oxo-bridges are in the range of 135.4(5)–136.2(8)°, substantially larger than those in dinuclear $[(dmtacn)_2Fe_2(O)(OOCMe)_2]^{2+}$ [120.0(2)°] but comparable to the 142.7(7)° value in $[Fe_4(bedda)_4(O)_2]$.^{10a} This means that, upon dimerization of the dinuclear Fe(III)–Fe(III) precursor, the μ -oxo-bridges adopt a more “open” configuration, reflecting also the constraints imposed by two carboxylato bridge moieties. The tetranuclear structure of **2** is quite unique and represents a new example of the binding versatility of carboxylates.

The ESI-MS spectrum of **2** in acetone shows the parent peak at m/z 575 ($[L_2Fe_2(O) + H + H_2O]^{3+}$), in line with the tetrameric iron(III) core rupture observed in the ESI-MS spectra for the analogous complexes.^{10a,25b} Absorptions at 753

(28) Neubold, P.; Wieghardt, K.; Nuber, B.; Weiss, J. *Inorg. Chem.* **1989**, *28*, 459–467.

(29) Romakh, V. B.; Therrien, B.; Labat, G.; Stoekli-Evans, H.; Shul'pin, G. B.; Süß-Fink, G. *Inorg. Chim. Acta* **2006**, *359*, 3297–3305.

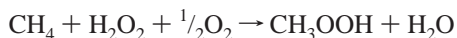
Table 2. Oxidation of Methane in D₂O Catalyzed by **1** and **2**^a

catalyst	TON in water							
	50 °C		60 °C		70 °C		80 °C	
	MeOH/ MeOOH/ HCOOH	Σ	MeOH/ MeOOH/ HCOOH	Σ	MeOH/ MeOOH/ HCOOH	Σ	MeOH/ MeOOH/ HCOOH	Σ
1	1.7/1.3/0	3	2/2/0	4	6.5/8.5/0	15	5/13/0	18
2	3.5/6.5/0	10	8/11/0	19	8/3/11	22	15/9/0	24
2 /pcaH	5/6/0	11	10/3/28	41	8/6/14	28	8/3/14	25

^a Conditions: 10⁻⁴ M catalyst, 0.50 M H₂O₂, 10 bar of air, 50 bar of methane, TON = catalyst turnover number, moles of product(s) per mole of catalyst after 4 h of the reaction. Product distribution contains MeOH/MeOOH/HCOOH ratios in the catalyst turnover numbers after 4 h of the reaction; [pcaH] = 1.6 × 10⁻³ M.

and 773 cm⁻¹, observed in the infrared spectrum, can be ascribed to the asymmetric Fe–O–Fe stretch modes, which are shifted to high values compared with those for the dinuclear complexes [(dmtacn)₂Fe₂(O)(OOCMe)₂]²⁺ (725 cm⁻¹) and [(dmtacn)₂Fe₂(O)(OOCPh)₂]²⁺ (724 cm⁻¹).²⁹ This can be rationalized by the fact that the energy of vibration increases as the Fe–O–Fe angle increases.^{10c,30} Therefore, in the more “open” configuration of **2**, these resonances should have higher values. The ν_{as}(C–O) stretching frequency for **2** is observed at 1622 cm⁻¹, while the ν_s(C–O) frequency appears at 1407 cm⁻¹.

Methane Oxidation in Water. The oxidation of methane (50 bar) is carried out in the 100 mL stainless steel autoclave equipped with a glass reactor in the presence of air (10 bar), using D₂O as the solvent. Both, the dinuclear and tetranuclear iron(III) complexes **1** and **2** have been used as catalysts.



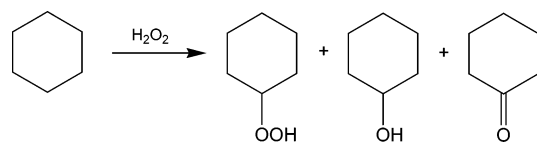
The product distribution was analyzed by ¹H NMR (MeCN as internal standard) and confirmed by GC analysis performed after reduction of the reaction mixture with NaBH₄ (*i*-PrOH as internal standard). Since no formaldehyde has been detected (Nash reagent³¹), we present the data for methanol, methyl hydroperoxide, and formic acid accumulation after 4 h. The results are summarized in Table 2.

Both **1** and **2** catalyze the oxidation of methane in water without any cocatalyst. Since **2** is more robust than **1**, it catalyzes the methane oxygenation more efficiently (Figure 1S); this effect is especially pronounced at moderate temperatures of 50–60 °C. However, at higher temperatures, **1** and **2** show comparable activities; the tetrameric structure

of **2** presumably undergoes decomposition, and the oxygenase activity of both catalysts is comparable.

In the presence of pyrazine-2-carboxylic acid (pcaH) as cocatalyst, the oxygenase activity of complex **2** increases (Figure 2S), which is in agreement with a reduced catalase activity of **2** under these conditions observed in the isopropanol oxidation. This effect is more pronounced at 60 °C; however, at higher temperatures, pcaH is not stable under the catalytic conditions, and the oxygenase activities of both systems become close. In the presence of pcaH as cocatalyst, the main oxidation product is formic acid, while without a cocatalyst the main oxidation products are methanol and methyl hydroperoxide.

Oxidation of Higher Alkanes. Higher alkanes are more easily oxidized than methane, and liquid alkanes can be handled without an autoclave, but for solubility reasons acetonitrile must be used as solvent instead of water. We studied at first the oxidation of cyclohexane with hydrogen peroxide catalyzed by **1** and **2** in acetonitrile solution at 25 °C.



In the case of **1**, the oxidation takes place during the initial period of 15 min, cyclohexyl hydroperoxide being the major product of the reaction (curve 1, Figure 4). However, after this period the oxygenase activity of the complex is blocked, and a slow decomposition of cyclohexyl hydroperoxide into the mixture of cyclohexanol (curve 2) and cyclohexanone (curve 3) is observed. Presumably, this decomposition is catalyzed by an iron complex generated from **1** in the course of the reaction; cyclohexanol is predominantly formed with an alcohol/ketone ratio of about 10, and the total catalyst turnover number attains 13.

Since the electronic spectra of the catalytic mixture do not change much (Figure 5), we assume **1** to be slightly modified, presumably, the μ-acetato bridge being exchanged by water/solvent molecules. Diaqua Fe(III)–Fe(III) complexes with similar tetradentate ligands have been isolated^{25b} and postulated as the intermediates for the dimerization process and for the catalytic oxidation with hydrogen peroxide.^{10a,10s,25b}

With **2**, the oxidation of cyclohexane possesses the same features as in the case of **1**, but the catalyst intermediate is more robust and maintains the oxygenase activity for at least 6 h of the reaction at 25 °C (Figure 6). Cyclohexyl hydroperoxide is the major oxygenation product in the initial period of the reaction (curve 1), while it slowly decomposes in the course of the reaction to give the mixture of cyclohexanol (curve 2) and cyclohexanone (curve 3) in the presence of an iron complex generated from **2**. Cyclohexanol is the predominant product after 6 h of reaction. The alcohol/ketone ratio decreases to 6, which could indicate that the catalytically active species are also involved in the oxidation of cyclohexanol to give cyclohexanone. The total catalyst

(30) Sanders-Loehr, J.; Wheeler, W. D.; Shiemke, A. K.; Averill, B. A.; Loehr, T. M. *J. Am. Chem. Soc.* **1989**, *111*, 8084–8093.

(31) Nash, T. *Biochem. J.* **1953**, *55*, 416–421.

(32) (a) Shul'pin, G. B.; Guerreiro, M. C.; Schuchardt, U. *Tetrahedron* **1996**, *52*, 13051–13062. (b) Shul'pin, G. B.; Kozlov, Y. N.; Nizova, G. V.; Süß-Fink, G.; Stanislas, S.; Kitaygorodskiy, A.; Kulikova, V. S. *J. Chem. Soc., Perkin Trans. 2* **2001**, 1351–1371. (c) Kozlov, Y. N.; Nizova, G. V.; Shul'pin, G. B. *J. Mol. Catal. A: Chem.* **2005**, *227*, 247–253.

(33) Deno, N. C.; Jedziniak, E. J.; Messer, L. A.; Meyer, M. D.; Stroud, S. G.; Tomczko, E. S. *Tetrahedron* **1977**, *33*, 2503–2508.

(34) (a) Lindsay Smith, J. R.; Shul'pin, G. B. *Tetrahedron Lett.* **1998**, *39*, 4909–4912. (b) Shul'pin, G. B.; Nizova, G. V.; Kozlov, Y. N.; Pechenkina, I. G. *New J. Chem.* **2002**, *26*, 1238–1245. (c) Shul'pin, G. B.; Nizova, G. V.; Kozlov, Y. N.; Arutyunov, V. S.; dos Santos, A. C. M.; Ferreira, A. C. T.; Mandelli, D. *J. Organomet. Chem.* **2005**, *690*, 4498–4504.

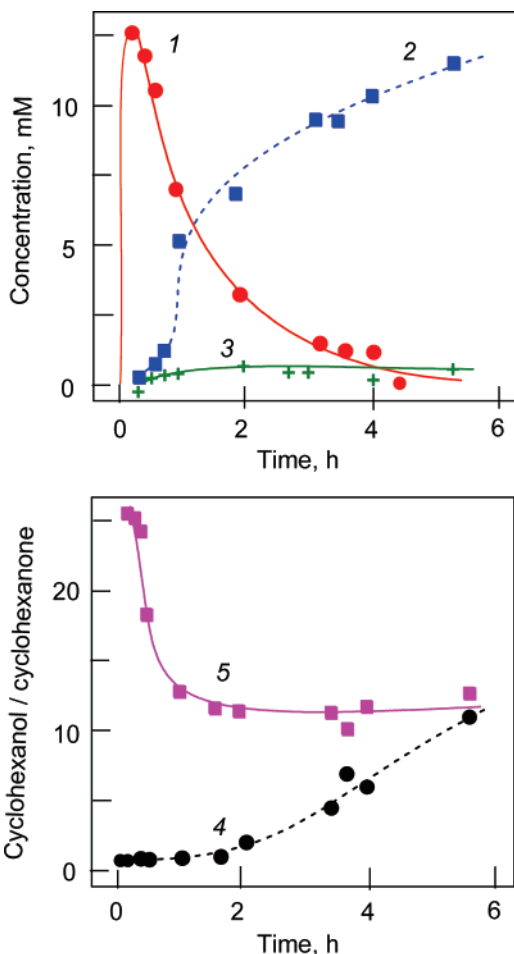


Figure 4. Oxidation of cyclohexane (0.46 M) with H_2O_2 (0.6 M) in MeCN at 25 °C catalyzed by complex **1** (1 mM). The following curves are shown: accumulation of cyclohexyl hydroperoxide (curve 1), cyclohexanol (2), and cyclohexanone (3), as well as the alcohol/ketone ratio measured before (4) and after (5) the reduction of the samples with triphenylphosphine.

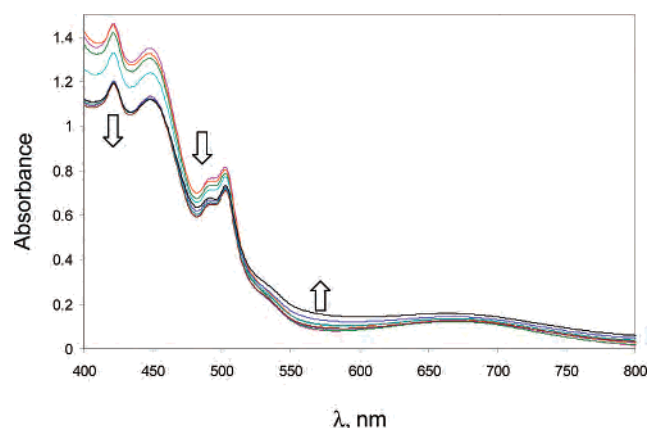


Figure 5. Oxidation of cyclohexane (0.46 M) with H_2O_2 (0.6 M) in MeCN at 25 °C catalyzed by **1** (1 mM) (electronic spectra of the catalytic reaction mixture (0–4 h)).

turnover number attains 43 and is significantly higher than that of **1** (TON = 13) and a recently reported Fe(III) tetramer (TON = 6.5).^{10s} Interestingly, pyrazine-2,3-dicarboxylic acid present in the solution inhibits the cyclohexane oxidation, which is different than the findings for the cyclohexane oxidation catalyzed by $[Fe_2(hptb)(\mu-OH)(NO_3)_2]^{2+}$ (hptb = *N,N,N',N'*-tetrakis(2-benzimidazolylmethyl)-2-hydroxy-1,3-

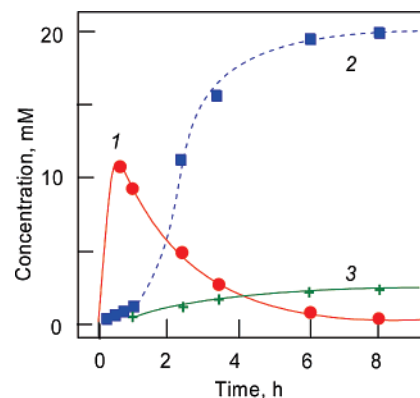


Figure 6. Oxidation of cyclohexane (0.46 M) with H_2O_2 (0.6 M) in MeCN at 25 °C catalyzed by **2** (0.5 mM). The following curves are shown: accumulation of cyclohexyl hydroperoxide (curve 1), cyclohexanol (2), and cyclohexanone (3).

diaminopropane),^{10h} which dramatically accelerated in the presence of pcaH (Table 3, entry 3).

The electronic spectra of **2** in the presence of H_2O_2 and cyclohexane are shown in Figure 7. The conversion of **2** into an intermediate iron(III) complex is almost completed after 2 h of the reaction. This intermediate has no oxygenase activity: the addition of a new portions of H_2O_2 results in no subsequent product formation but instead in H_2O_2 decomposition and further complex degradation.

To elucidate the nature of the oxidizing species generated from **1** and **2** upon addition of hydrogen peroxide, we studied the oxidation of higher linear and branched alkanes (*n*-hexane, *n*-heptane, *n*-octane, and isooctane). The selectivity parameters are given in Table 3. All parameters were measured after reduction of the reaction mixtures with triphenylphosphine before the GC analysis and were calculated using the ratios of isomeric alcohols. The parameter $C(1)/C(2)/C(3)/C(4)$ indicates the relative normalized reactivities of hydrogen atoms at carbons 1, 2, 3, and 4 of the chain of unbranched alkanes (i.e., calculated taking into account the number of hydrogen atoms at each carbon). The parameter $1^\circ/2^\circ/3^\circ$ indicates the relative normalized reactivities of hydrogen atoms at primary, secondary, and tertiary carbons of isooctane.

A comparison of the selectivity parameters (Table 3) shows that **1** and **2** are only slightly more selective for the oxidation of the different C–H bonds than known hydroxyl radical-generating systems (photochemical H_2O_2 decomposition, Fenton reagent, vanadate/pcaH), suggesting a radical pathway in the case of **1** and **2** ($C(2)/C(1) < 20$). The higher tendency to discriminate between primary and secondary hydrocarbon bonds may be explained by the assumption that a more selective oxygen-centered radical (ferroxy radical, alkoxy radical), rather than HO^\bullet radicals alone, act as the active species.

In the isooctane molecule, the secondary C–H bonds are surrounded by bulky *t*-butyl and *i*-propyl groups, and the selectivity parameter $C(2)/C(1)$ in linear alkanes compared to $2^\circ/1^\circ$ for isooctane reflects the steric hindrance for the oxidizing species. Given that the parameters $[C(2)/C(1)]/[2^\circ/1^\circ]$ for **1** and **2** complexes are similar to those for hv–

Table 3. Selectivity Parameters in Oxidation of Alkanes in Acetonitrile^a

entry	system	C(1)/C(2)/C(3)/C(4)			1°/2°/3°	trans/cis	
		<i>n</i> -hexane	<i>n</i> -heptane	<i>n</i> -octane	isooctane	<i>cis</i> -DMCH	<i>trans</i> -DMCH
1	1 -H ₂ O ₂ (25 °C)	1:13:13	1:10:10:6	1:8:9:7	1:2:21	1.6	1.2
2	2 -H ₂ O ₂ (25 °C)	1:13:13	1:15:14:11	1:10:12:9	1:5:11	0.9	1.3
3	Fe ₂ (HPTB)-pcaH-H ₂ O ₂ (25 °C) ^b		1:6:6:5		1:4:8	3.5 ^c	5.1 ^c
4	hn-H ₂ O ₂ (20 °C)	1:10:7	1:7:6:7		1:2:6	0.9	1.0
5	FeSO ₄ -H ₂ O ₂ (20 °C)		1:5:5:5		1:3:6	1.3	1.2
6	<i>n</i> -Bu ₄ NVO ₃ -pcaH-H ₂ O ₂ (40 °C) ^d	1:7:7	1:6:7:5	1:7:8:6	1:1:17	0.75	0.8
7	H ₂ O ₂ in CF ₃ COOH ^e	1:364:363			1:52:0		
8	[(tmtacn) ₂ Mn ₂ O ₃] ²⁺ -MeCOOH-H ₂ O ₂ (20 °C) ^f		1:46:35:35		1:8:40	0.34	4.1

^a All parameters were measured after reduction of the reaction mixtures with triphenylphosphine before GC analysis and calculated based on the ratios of isomeric alcohols. Parameter C(1)/C(2)/C(3)/C(4) is relative normalized (i.e., calculated taking into account the number of hydrogen atoms at each carbon) reactivities of hydrogen atoms at carbons 1, 2, 3, and 4 of the chain of unbranched alkanes. Parameter 1°/2°/3° is relative normalized reactivities of hydrogen atoms at primary, secondary, and tertiary carbons of branched alkanes. Parameter trans/cis is the ratio of trans and cis isomers of *tert*-alcohols formed in the oxidation of *cis*- or *trans*-disubstituted cyclohexanes. *cis*-DMCH and *trans*-DMCH are *cis*-1,2-dimethylcyclohexane and *trans*-1,2-dimethylcyclohexane, respectively. ^b Catalyst [Fe₂(hptb)(μ-OH)(NO₃)₂](NO₃)₂·CH₃OH·2H₂O, see ref 10h. ^c Corresponding isomers of decalin were used instead of 1,2-dimethylcyclohexanes. ^d For this system, see ref 32. ^e See ref 33. ^f For this system, see ref 34.

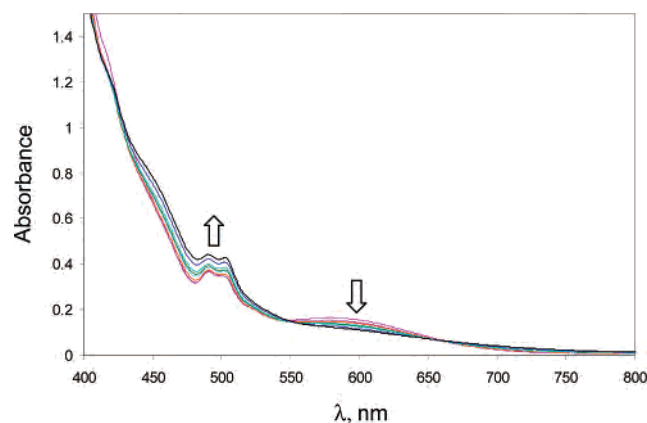


Figure 7. Oxidation of cyclohexane (0.46 M) with H₂O₂ (0.6 M) in MeCN at 25 °C catalyzed by **2** (0.5 mM) (electronic spectra of the catalytic reaction mixture (0–6 h)).

H₂O₂ system, we can assume that the oxidizing species generated from **1** and **2** have minimal steric restrictions and are situated on the surface of the complexes or, once generated, escape the catalyst and attack the substrate from the solvent cage. This is also consistent with the fact that, in the oxidation of *cis*- and *trans*-1,2-dimethylcyclohexane with H₂O₂ catalyzed by **1** and **2**, no stereoselectivity has been observed.

Oxidation of Isopropanol. We also studied the catalytic activity of **1** and **2** for the oxidation of isopropanol with hydrogen peroxide to give acetone. The reaction was carried out in aqueous solution or acetonitrile in the absence and in the presence of ascorbic (ascH) or pyrazine-2-carboxylic acid (pcaH) at 20 °C. The results are shown in Table 4.

The highest catalytic activity was observed for [L₄Fe₄(O)₂]⁴⁺ (**2**) in the presence of pcaH in water, the TON being 463 after 1 h at 20 °C. If added to the catalytic mixture, pcaH significantly suppresses the catalase activity of **1** and **2**, apparently it acts as a co-ligand to the iron centers. Surprisingly, the oxidation activity of **1** and **2** are close, regardless of the difference in the number of iron centers per molecule. Both complexes are much more active in water than in acetonitrile solution.

In aqueous solution, **1** and **2** efficiently catalyze isopropanol oxidation without any cocatalyst added because of the

Table 4. Oxidation of Isopropanol in Water and Acetonitrile, Catalyzed by Complexes **1** and **2** in the Absence or Presence of 0.001 M Pyrazine-2-carboxylic Acid (pcaH) or 0.01 M Ascorbic Acid (ascH) as Cocatalyst^a

catalyst	TON (after 1 h) in water			TON (after 1 h) in acetonitrile		
	without cocatalyst	with pcaH	with ascH	without cocatalyst	with pcaH	with ascH
FeCl ₂	5	56	243	2	26	37
1	190	431	268	16	9	42
2	226	463	301	26	19	40

^a Conditions: 20 °C, 1 h, 1.0 × 10⁻⁴ M FeCl₂, **1**, **2**, 0.20 M isopropanol, 0.50 M H₂O₂.

presence of the pendent acetato arm within the macrocyclic ligand. Indeed, complexes [(dmtacn)₂Fe₂(O)(OOCMe)₂]²⁺ and [(dmtacn)₂Fe₂(O)(OOCPh)₂]²⁺, containing only bridging carboxylato groups, are almost inactive in the absence of cocatalyst.²⁹ With ascorbic acid as cocatalyst **1**, **2**, and [(dmtacn)₂Fe₂(O)(OOCMe)₂]²⁺, as well as iron(II) chloride, give comparable TONs, regardless of the nature and the quantity of iron centers.²⁹ Therefore, we can assume that in the oxidation of isopropanol ascH acts preferentially as a stoichiometric reducing agent.

Conclusion

We have developed a new 1,4,7-triazacyclononane macrocycle containing a carboxylato function in the side arm at one of the nitrogen atoms. Two new iron(III) complexes containing the 2-(4,7-dimethyl-1,4,7-triazacyclononan-1-yl)-acetate ligand (L) have been synthesized. While **1** represents a dinuclear Fe(III)–Fe(III) complex, [(N₃O-L)₂Fe₂(μ-O)(μ-OOCMe)]⁺, with pendent carboxylato arms being monodentately coordinated to iron(III) centers, **2** is a tetranuclear complex, [(N₃O₂-L)₄Fe₄(O)₂]⁴⁺; the bidentate mode of pendent acetato arms coordination bridging two dimeric subunits into a “dimer of dimers” has been observed. The tetranuclear structure of **2** represents a new example of the binding versatility of carboxylates.

Complexes **1** and **2** show significant catalytic oxygenase activity in the oxidation of alcohols and alkanes with H₂O₂; without the addition of cocatalyst, the reaction proceeds under mild conditions. The addition of an amino acid (pcaH) decreases the catalase activity of these complexes in aqueous

Tetrairon Complex $[Fe_4(N_3O_2-L)_4(\mu-O)_2]^{4+}$

solution, improving the catalytic performance in the oxidation of isopropanol. The tetrameric **2** complex is more robust than the dimeric **1** complex and maintains the oxygenase activity for hours under catalytic conditions at room temperature. The selectivity pattern in the oxidation of linear and branched alkanes catalyzed by **1** and **2** complexes suggests the oxidizing species to have a radical character, tentatively assumed to be a ferroxyl radical or diffusively free oxygen radical species operating at the expense or in parallel with the hydroxyl radicals. Since both complexes have structural and selectivity features close to those observed for sMMO, we used **1** and **2** for the oxygenation of methane with H_2O_2 in aqueous solution. We found that both complexes are active in this reaction under moderate temperatures (50–80 °C)

and pressures (60 bar). Finally, **1** and **2** can be used for the oxidation of alkanes and alcohols with H_2O_2 without the addition of reducing agents or co-ligands.

Acknowledgment. The authors are grateful to the Suisse National Science Foundation (Grant 200020-109129) for financial support and Professor Helen Stoeckli-Evans (University of Neuchatel) for the access to the X-ray facilities.

Supporting Information Available: Figures 1S and 2S and crystallographic data for complex [**2**][PF₆]₄·5MeCN in CIF format. This material is available free of charge via the Internet at <http://pubs.acs.org>.

IC062207K